Size-Selective Transport of Uncharged Solutes through Multilayer Polyelectrolyte Membranes

Xiaoyun Liu and Merlin L. Bruening*

Department of Chemistry, Michigan State University, East Lansing, Michigan 48824

Received July 1, 2003. Revised Manuscript Received November 15, 2003

Several recent studies demonstrated highly selective ion transport through multilayer polyelectrolyte membranes. This paper examines the transport of neutral molecules through multilayer polyelectrolyte films and shows significant size-based discrimination among organic analytes. Simple 7-bilayer poly(styrene sulfonate) (PSS)/poly(allylamine hydrochloride) (PAH) films deposited on porous alumina exhibit a glucose/sucrose selectivity of ∼150 in both diffusion dialysis and nanofiltration. However, selectivity among smaller solutes is fairly low (methanol/glycerol ≈ 2 and glycerol/glucose ≈ 8). Because inorganic ions are generally smaller than glycerol, these results suggest that size-based selectivity in ion transport through PSS/PAH films is minimal. High selectivity in nanofiltration by PSS/PAH membranes is accompanied by relatively high solute rejections. For example, 7-bilayer PSS/PAH membranes exhibit a methanol rejection of 70% and a sucrose rejection of >99.9%. Although such high rejections will preclude the use of these membranes in sugar separations, they will allow removal of organic pollutants from water. The high water flux through PSS/PAH films (0.9 $m^3m^{-2}d^{-1}$ at 4.8 bar) would also be important in water purification. Capping PSS/PAH films with a few bilayers of poly(acrylic acid) (PAA)/PAH increases glycerol/glucose diffusion-dialysis selectivity from 8 to 75. Thus, controlling film composition allows tailoring of membrane properties. Simulations of nanofiltration and diffusion dialysis data for 7-bilayer PSS/PAH membranes suggest that these films have pores with radii of 0.4−0.5 nm.

Introduction

Nanofiltration (NF) is becoming increasingly important for separations in areas such as water purification, treatment of pulp and paper mill effluents, fractionation/purification of protein, cheese-whey desalting, and sulfate removal from oil-well injection water.[1] The separation mechanism in NF can involve both steric (sieving) and electrical (Donnan) effects, and the advantage of NF over reverse osmosis (RO) is operation at moderate pressure with a relatively high flux. However, analytes separated by NF are generally larger than those separated by RO.

The key to further enhancing the utility of NF is the development of membranes that exhibit high flux and selectivity as well as durability and resistance to fouling.[2,3] Synthesis of such membranes typically requires formation of an ultrathin, defect-free film on a highly permeable support.[4−8] The support affords mechanical stability while the dense membrane "skin" provides selectivity. Although the skin is much less permeable than the support, its minimal thickness still allows high flux.

Several recent studies suggest that alternating adsorption of polycations and polyanions is a promising method for fabrication of selective, ultrathin membrane skins on porous supports.[9−16] The films prepared by this method are attractive materials for membrane skins for several reasons. First, their minimal thickness should allow high fluxes.[17] Film thickness can be controlled on the nanometer scale simply by varying the number of deposited bilayers. Second, nearly any polyelectrolyte can form these films, and thus one can easily tune a separation through proper selection of film constituents.[18−25] In addition, variation of deposition conditions such as solution pH [26−28] and supporting electro-

* To whom correspondence should be addressed. Phone: 517-355-9715, ext 237. Fax: 517-353-1793. E-mail: bruening@cem.msu.edu.

(1) Xu, Y.; Lebrun, R. E. *Desalination* **1999**, *122*, 95−106.
(2) Van den Berg, G. B.; Smolders, C. A. *J. Membr. Sci.* **1989**, *40*, 149−172.
(3) Nakao, S.; Wijmans, J. G.; Smolders, C. A. *J. Membr. Sci.* **1986**, *26*, 165−178.
(4) Kesting, R. E.; Fritzche, A. K. *Polymeric Gas Separation Membranes*; John Wiley & Sons: New York, 1993.
(5) Pinnau, I.; Koros, W. J. *Ind. Eng. Chem. Res.* **1991**, *30*, 1837−1840.
(6) Pinnau, I.; Koros, W. J. *J. Appl. Polym. Sci.* **1992**, *46*, 1195−1204.
(7) Ding, Y.; Bikson, B.; Nelson, J. K. *Macromolecules* **2002**, *35*, 912−916.
(8) Clausi, D. T.; Koros, W. J. *J. Membr. Sci.* **2000**, *167*, 79−89.
(9) Stroeve, P.; Vasquez, V.; Coelho, M. A. N.; Rabolt, J. F. *Thin Solid Films* **1996**, *284−285*, 708−712.
(10) Leväsalmi, J. M.; McCarthy, T. J. *Macromolecules* **1997**, *30*, 1752−1757.
(11) Kotov, N. A.; Magonov, S.; Tropsha, E. *Chem. Mater.* **1998**, *10*, 886−895.
(12) Schlenoff, J. B.; Ly, H.; Li, M. *J. Am. Chem. Soc.* **1998**, *120*, 7626−7634.
(13) Krasemann, L.; Tieke, B. *Langmuir* **2000**, *16*, 287−290.
(14) Harris, J. J.; Stair, J. L.; Bruening, M. L. *Chem. Mater.* **2000**, *12*, 1941−1946.
(15) Dubas, S. T.; Farhat, T. R.; Schlenoff, J. B. *J. Am. Chem. Soc.* **2001**, *123*, 5368−5369.
(16) Jin, W.; Toutianoush, A.; Tieke, B. *Langmuir* **2003**, *19*, 2550−2553.
(17) Liu, C.; Martin, C. R. *Nature* **1991**, *352*, 50−52.
(18) von Klitzing, R.; Möhwald, H. *Thin Solid Films* **1996**, *352*, 284−285.

10.1021/cm034559k CCC: $27.50
Published on Web 12/23/2003

lyte concentration [29−32] also allows optimization of film properties. Finally, recent studies suggest that some polyelectrolyte films resist cell growth and protein adhesion and thus may be somewhat resistant to fouling.[33−37]

Multilayer polyelectrolyte membranes (MPMs) are especially attractive for separating ions with different valences.[13,14,38] Krasemann and Tieke demonstrated Cl^-/SO_4^{2-} selectivity as high as 45 using poly(allylamine hydrochloride) (PAH)/poly(styrene sulfonate) (PSS) films and suggested that selectivity is due to greater Donnan exclusion of the divalent SO_4^{2-}.[13] Farhat and Schlenoff showed that diffusion through multilayer polyelectrolyte films on electrodes depends on analyte charge,[39,40] and we recently reported enhancement of the ion-transport selectivity of MPMs through cross-linking, hybridization, and control over charge density.[41−44] Preliminary simulations suggest that both selective diffusion and Donnan exclusion play a role in effecting selectivity.

The main objective of this work is to better understand transport through multilayered polyelectrolyte films by studying the movement of various neutral molecules across MPMs. The use of neutral analytes eliminates Donnan effects and allows us to focus exclusively on size-based selectivity. In addition to providing fundamental insight, neutral molecule studies will be important for potential applications of MPMs such as controlled release,[45−50] water purification,[51,52] and salt/sugar separations.[53,54] We chose to investigate transport of methanol, glycerol, glucose, and sucrose because these molecules differ in size (Table 1) and yet have similar functional groups and hydrophilicities.[55,56] Diffusion dialysis studies with these molecules show that MPMs can exhibit very high size-based selectivities (glucose/sucrose selectivity reaches 150) that depend on membrane composition. Selectivities are maintained in high-flux NF, but rejections are also high. Even with the smallest molecule, methanol, rejection by PSS/PAH films is 70%, i.e., the permeate concentration is 30% of that in the feed. These high rejections suggest that PSS/PAH membranes may be useful in removal of organic pollutants from water.

Table 1. Molecular Weights, Diffusion Coefficients (D), and Stokes' Radii (r_s) of Several Neutral Solutes[55,57]

solute	MW	D ($m^2s^{-1} \times 10^{-9}$)	r_s (nm)
methanol	32	1.56	0.157
glycerol	92	0.95	0.260
glucose	180	0.69	0.355
sucrose	342	0.52	0.471

Experimental Section

Materials. Poly(styrene sulfonate) (PSS, Aldrich, M_w = 70 000), poly(allylamine hydrochloride) (PAH, Aldrich, M_w = 70 000), poly(acrylic acid) (PAA, M_w = 90 000, 25 wt % solution, Alfa Aesar), $MnCl_2$ (Mallinckrodt), NaBr (Aldrich), NaCl (Mallinckrodt), methanol (CCI, ACS grade, anhydrous), glycerol (CCI, ACS grade, anhydrous), glucose (Aldrich), and sucrose (Aldrich) were used as received. The porous alumina supports (Anodisc 0.02-μm membrane filters) were purchased from Whatman and subjected to UV/O_3 cleaning (Boekel UV-Clean model 135500) for 15 min before film deposition. Deionized water (Milli-Q, 18.2 MΩcm) was used for rinsing and preparation of the polyelectrolyte solutions. The pH of polyelectrolyte solutions was adjusted with dilute NaOH or HCl.

Film Deposition. A cleaned porous alumina support was first placed in an O-ring holder so that only the top of the substrate would be exposed to polyelectrolyte solutions. Polyelectrolyte deposition began with immersion of the alumina support in 0.02 M PSS (pH 2.1, 0.5 M $MnCl_2$) for 2 min (polymer concentrations are always given with respect to the repeating unit.) The substrate was rinsed with deionized water for 1 min before a 5-min immersion in 0.02 M PAH (pH 2.3, 0.5 M NaBr for PSS/PAH layers and pH 4.5, 0.5 M NaCl for PAA/PAH layers) and subsequent rinsing. Additional bilayers were deposited similarly. Supporting electrolytes and pH values were chosen to follow literature procedures.[28,58] Capped films were synthesized through deposition of a 5-bilayer PSS/

(19) Han, S.; Lindholm-Sethson, B. *Electrochim. Acta* **1999**, *45*, 845−853.
(20) Ichinose, I.; Mizuki, S.; Ohno, S.; Shiraishi, H.; Kunitake, T. *Polym. J.* **1999**, *31*, 1065−1070.
(21) Delcorte, A.; Bertrand, P.; Wischerhoff, E.; Laschewsky, A. *Langmuir* **1997**, *13*, 5125−5136.
(22) Möhwald, H. *Colloids Surf., A* **2000**, *171*, 25−31.
(23) Lvov, Y.; Ariga, K.; Ichinose, I.; Kunitake, T. *J. Am. Chem. Soc.* **1995**, *117*, 6117−6123.
(24) Russell, R. J.; Sirkar, K.; Pishko, M. V. *Langmuir* **2000**, *16*, 4052−4054.
(25) Caruso, F.; Niikura, K.; Furlong, D. N.; Okahata, Y. *Langmuir* **1997**, *13*, 3422−3426.
(26) Mendelsohn, J. D.; Barrett, C. J.; Chan, V. V.; Pal, A. J.; Mayes, A. M.; Rubner, M. F. *Langmuir* **2000**, *16*, 5017−5023.
(27) Shiratori, S. S.; Rubner, M. F. *Macromolecules* **2000**, *33*, 4213−4219.
(28) Yoo, D.; Shiratori, S. S.; Rubner, M. F. *Macromolecules* **1998**, *31*, 4309−4318.
(29) Harris, J. J.; Bruening, M. L. *Langmuir* **2000**, *16*, 2006−2013.
(30) Ladam, G.; Schaad, P.; Voegel, J. C.; Schaaf, P.; Decher, G.; Cuisinier, F. *Langmuir* **2000**, *16*, 1249−1255.
(31) Lösche, M.; Schmitt, J.; Decher, G.; Bouwman, W. G.; Kjaer, K. *Macromolecules* **1998**, *31*, 8893−8906.
(32) Steitz, R.; Leiner, V.; Siebrecht, R.; von Klitzing, R. *Colloids Surf., A* **2000**, *163*, 63−70.
(33) Mendelsohn, J. D.; Yang, S. Y.; Hiller, J. A.; Hochbaum, A. I.; Rubner, M. F. *Biomacromolecules* **2003**, *4*, 96−106.
(34) Yang, S. Y.; Mendelsohn, J. D.; Rubner, M. F. *Biomacromolecules* **2003**, *4*, 987−994.
(35) Müller, M.; Rieser, T.; Dubin, P. L.; Lunkwitz, K. *Macromol. Rapid Commun.* **2001**, *22*, 390−395.
(36) Meier-Haack, J.; Müller, M. *Macromol. Symp.* **2002**, *188*, 91−103.
(37) Ladam, G.; Schaaf, P.; Cuisinier, F. J. G.; Decher, G.; Voegel, J.-C. *Langmuir* **2001**, *17*, 878−882.
(38) Sullivan, D. M.; Bruening, M. L. *J. Am. Chem. Soc.* **2001**, *123*, 11805−11806.
(39) Farhat, T. R.; Schlenoff, J. B. *Langmuir* **2001**, *17*, 1184−1192.
(40) Farhat, T. R.; Schlenoff, J. B. *J. Am. Chem. Soc.* **2003**, *125*, 4627−4636.
(41) Stair, J. L.; Harris, J. J.; Bruening, M. L. *Chem. Mater.* **2001**, *13*, 2641−2648.
(42) Dai, J.; Jensen, A. W.; Mohanty, D. K.; Erndt, J.; Bruening, M. L. *Langmuir* **2001**, *17*, 931−937.
(43) Balachandra, A. M.; Dai, J.; Bruening, M. L. *Macromolecules* **2002**, *35*, 3171−3178.
(44) Dai, J.; Balachandra, A. M.; Lee, J. I.; Bruening, M. L. *Macromolecules* **2002**, *35*, 3164−3170.
(45) Caruso, F.; Yang, W.; Trau, D.; Renneberg, R. *Langmuir* **2000**, *16*, 8932−8936.
(46) Shi, X.; Caruso, F. *Langmuir* **2001**, *17*, 2036−2042.
(47) Qiu, X.; Leporatti, S.; Donath, E.; Möhwald, H. *Langmuir* **2001**, *17*, 5375−5380.
(48) Duchesne, T. A.; Brown, J. Q.; Guice, K. B.; Lvov, Y.; McShane, M. J. *Sens. Mater.* **2002**, *14*, 293−308.
(49) Lvov, Y.; Antipov, A. A.; Mamedov, A.; Möhwald, H.; Sukhorukov, G. B. *Nano Lett.* **2001**, *1*, 125−128.
(50) Kato, N.; Schuetz, P.; Fery, A.; Caruso, F. *Macromolecules* **2002**, *35*, 9780−9787.
(51) Bohdziewicz, J.; Bodzek, M.; Wasik, E. *Desalination* **1999**, *121*, 139−147.
(52) Yaroshchuk, A.; Staude, E. *Desalination* **1992**, *86*, 115−134.
(53) Matsubara, Y.; Iwasaki, K.; Nakajima, M.; Nabetani, H.; Nakao, S. *Biosci. Biotechnol. Biochem.* **1996**, *60*, 421−428.
(54) Wang, X.; Zhang, C.; Ouyang, P. *J. Membr. Sci.* **2002**, *204*, 271−281.
(55) Bowen, W. R.; Mohammad, A. W.; Hilal, N. *J. Membr. Sci.* **1997**, *126*, 91−105.
(56) Bowen, W. R.; Mohammad, A. W. *AIChE J.* **1998**, *44*, 1799−1812.

PAH film followed by deposition of PAA/PAH. The PAA deposition step involved a 5-min immersion in 0.02 M PAA (pH 4.5, 0.5 M NaCl). Films were dried with N_2 only after deposition of all layers.

Transport Studies. A home-built dialysis apparatus was used to study the transport of neutral molecules. The apparatus consisted of two glass cells (100 mL) connected by a 2.5-cm-long neck in which the membrane was sandwiched between the feed and permeate sides. The exposed membrane area was 2.3 cm^2, and both feed and permeate sides were stirred vigorously to minimize concentration polarization at the membrane interface. (Increasing the stirring speed does not enhance transport, suggesting that boundary layers in solution do not significantly affect flux. This probably stems from the fact that the porous alumina support is 60 μm thick, so resistance to mass transport in the support is much larger than that in the boundary layers.) The permeate side was initially filled with deionized water, and the feed side contained 0.2 M methanol and 0.005 M glycerol, 0.005 M glycerol and 0.005 M glucose, or 0.005 M glucose and 0.05 M sucrose. Feed concentrations were chosen on the basis of fluxes and analysis limitations for each analyte. (Experiments with uncoated porous alumina employed lower analyte concentrations to avoid dilution prior to analysis: 0.1 M methanol, 0.0005 M glycerol, 0.0005 M glucose, and 0.0005 M sucrose.) Flux values were normalized by dividing them by the concentration in the feed side.

NF was performed using a cross-flow apparatus described previously.[59] The system was pressurized with Ar to 70 psi, and a centrifugal pump circulated the analyte solution through the system and across the membrane. The volume of the feed solution (2 L) was about 30× greater than that of the total permeate, so the feed composition (0.002 M methanol and 0.0001 M glycerol; or 0.0001 M glycerol, 0.0002 M glucose, and 0.005 M sucrose; or 0.0001 M glycerol, 0.0002 M glucose, and 0.025 M sucrose) was essentially constant. To avoid concentration polarization, the flow rate across the membrane was kept at 18 mL/min and monitored by a flowmeter located between the pump and membrane cell. The membrane area exposed to the analyte solution was 1.5 cm^2, and permeate was collected with a graduated cylinder after a 10-h equilibration period. Aliquots were taken at 30-min intervals for 1.5 h after the equilibration period, and no significant change in permeate composition was observed after an additional 6 h of NF.

Methanol was analyzed by gas chromatography (Shimadzu, GC-17A, Version 3) using a 30-m-long capillary column (Restek, RTX-BAC1, i.d. 0.53 mm, film thickness 3 μm). Glycerol, glucose, and sucrose were analyzed by liquid chromatography (Dionex, DX-600, CarbonPac PA-10 column, 100 mM NaOH eluent) coupled with integrated amperometric detection (Dionex, ED-50).

Results and Discussion

Diffusion Dialysis through PSS/PAH Membranes. To examine the selectivity of PSS/PAH films, we initially employed diffusion dialysis. In these experiments, a porous alumina substrate separates a permeate phase (initially deionized water) from an aqueous source phase that contains the analytes of interest. By monitoring analyte concentrations in the permeate phase as a function of time, one can measure the rate of transport across the membrane. Because analyte concentrations in the permeate phase are negligible compared to those in the source phase, the concentration gradients across the membrane are essentially constant, and permeate-phase concentrations increase linearly with time.

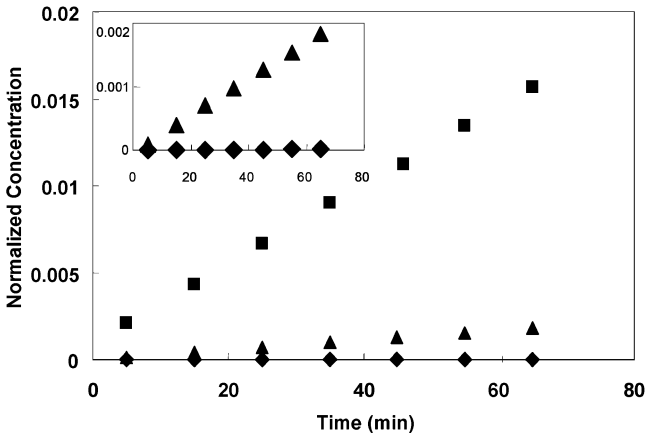

Figure 1. Normalized permeate-phase concentrations of glycerol (squares), glucose (triangles), and sucrose (diamonds) as a function of time in diffusion dialysis through a 7-bilayer PSS/PAH membrane. The inset shows an expanded view for glucose and sucrose. Concentrations were normalized by dividing by the source-phase concentration, and data are from experiments using feed solutions containing 0.005 M glycerol and 0.005 M glucose or 0.005 M glucose and 0.05 M sucrose. Glucose flux was similar for both feed solutions.

Figure 1 shows permeate-phase concentration as a function of time for the diffusion of glycerol, glucose, and sucrose through porous alumina coated with a 7-bilayer PSS/PAH film. Glycerol transport is about 8 times faster than glucose transport, and, remarkably, the flux of glucose across the membrane is 150-fold greater than that of sucrose (see Table 2). Corresponding selectivities for bare porous alumina are <1.5. As all of these analytes are neutral and hydrophilic, selectivity must be based primarily on size.

In ion transport through PSS/PAH films, terminating a membrane with PAH rather than PSS gives a 2-fold increase in the flux of SO_4^{2-} and $Ni(CN)_4^{2-}$ but has little effect on Cl^- transport.[14] In contrast, the flux of sucrose *decreases* 2-fold on going from a 6.5-bilayer ([PSS/PAH]$_6$PSS) to a 7-bilayer ([PSS/PAH]$_7$) film (Table 2), and the fluxes of glycerol and glucose also decrease slightly (~20%). The significant decrease in sucrose flux probably results from a tighter surface packing when the top layer is PAH.[59] Recent NMR studies also show that the composition of the top layer of a polyelectrolyte film affects the mobility of water within the film.[60] Polymer packing should have little effect on the transport of SO_4^{2-} and $Ni(CN)_4^{2-}$ because the Stokes' radii of these molecules are less than that of glycerol.[61] Thus, in the transport of divalent anions, changes in Donnan exclusion are the primary result of changing the surface layer to a polycation, and flux increases when terminating films with PAH. In contrast, with neutral molecules Donnan exclusion is not operative, and addition of a PAH layer yields a decrease in flux due to tighter packing and/or a thicker membrane.

Diffusion Dialysis through Hybrid PSS/PAH/PAA Membranes. Simple PSS/PAH membranes are highly selective for glucose over sucrose, but the selectivity for glycerol over glucose is fairly low. Our previous

(57) Derlacki, Z. J.; Easteal, A. J.; Edge, A. V. J.; Woolf, L. A. *J. Phys. Chem.* **1985**, *89*, 5318−5322.
(58) Decher, G.; Lvov, Y.; Schmitt, J. *Thin Solid Films* **1994**, *244*, 772−777.
(59) Stanton, B. W.; Harris, J. J.; Miller, M. D.; Bruening, M. L. *Langmuir* **2003**, *19*, 7038−7042.
(60) McCormick, M.; Smith, R. N.; Graf, R.; Barrett, C. J.; Reven, L.; Spiess, H. W. *Macromolecules* **2003**, *36*, 3616−3625.
(61) Sulfate has a Stokes' radius of 0.23 nm, and, on the basis of our previous studies of SO_4^{2-} and $Ni(CN)_4^{2-}$ transport through bare porous alumina, $Ni(CN)_4^{2-}$ should have a similar radius.[41]

Table 2. Normalized Fluxes (mol cm^{-2} s^{-1}/M) and Selectivities in Diffusion Dialysis through Bare Porous Alumina and Alumina Coated with Polyelectrolyte Films[a]

film composition	methanol flux	glycerol flux	glucose flux	sucrose flux	methanol/ glycerol	glycerol/ glucose	glucose/ sucrose
bare	3.6×10^{-7}	2.6×10^{-7}	1.8×10^{-7}	1.3×10^{-7}	1.36	1.45[b]	1.35
	(6×10^{-9})	(8×10^{-9})	(1×10^{-8})	(1×10^{-8})	(0.05)	(0.11)	(0.02)
[PSS/PAH]$_6$PSS	3.5×10^{-7}	2.1×10^{-7}	2.7×10^{-8}	3.4×10^{-10}	1.96	6.4	80
	(4×10^{-8})	(5×10^{-9})	(2×10^{-9})	(5×10^{-11})	(0.05)	(0.4)	(7)
[PSS/PAH]$_7$	3.0×10^{-7}	1.7×10^{-7}	2.2×10^{-8}	1.5×10^{-10}	2.0	7.8	150
	(1×10^{-8})	(5×10^{-9})	(2×10^{-9})	(4×10^{-11})	(0.1)	(0.9)	(40)
[PSS/PAH]$_5$	2.4×10^{-7}	7.3×10^{-8}	9.1×10^{-10}	$<4.5 \times 10^{-12}$	3.5	75	>200
[PAA/PAH]PAA	(2×10^{-8})	(6×10^{-9})	(3×10^{-11})		(0.6)	(20)	
[PSS/PAH]$_5$	2.8×10^{-7}	1.3×10^{-7}	1.4×10^{-8}	1.0×10^{-10}	2.35	10.2	133
[PAA/PAH]$_2$	(5×10^{-9})	(2×10^{-8})	(7×10^{-10})	(6×10^{-12})	(0.03)	(0.3)	(6)

[a] The values in parentheses represent the standard deviations of at least three measurements. [b] In this case, the selectivity was obtained by dividing the flux of glycerol (from the experiment with methanol/glycerol as the feed solution) by the flux of glucose (from the experiment with glucose and sucrose as the feed solution). In all other cases, analytes were examined competitively in the same solution, and selectivity values are an average of the selectivities in three experiments.

Table 3. Percent Rejections, Water Fluxes (in m^{3}m^{-2}d^{-1}), and Selectivities from NF Experiments with Multilayer Polyelectrolyte Membranes and Solutions Containing Several Neutral Molecules

film composition	methanol	glycerol	glucose	sucrose	water flux	glycerol/glucose	glucose/sucrose
[PSS/PAH]$_6$PSS		90.7 ± 0.4[a]	97.4 ± 0.6[a]	99.96 ± 0.01[a]	0.89 ± 0.05[a]	3.7 ± 0.7[a]	68 ± 5[a]
[PSS/PAH]$_7$		87 ± 3[a]	98.3 ± 0.2[a]	>99.99[a]	0.90 ± 0.08[a]	7.7 ± 0.9[a]	>100[a]
		97.4 ± 0.4[b]	99.1 ± 0.2[b]	99.99 ± 0.01[b]	0.70 ± 0[b]	2.8 ± 0.4[b]	144 ± 31[b]
	70 ± 5[c]	88 ± 2[c]			0.9 ± 0.1[c]		

[a] Experiment conducted with a feed solution containing 0.0001 M glycerol, 0.0002 M glucose, and 0.005 M sucrose. With 7-bilayer films, sucrose concentration in the permeate was near the instrument detection limit. [b] Experiment conducted with a feed solution containing 0.0001 M glycerol, 0.0002 M glucose, and 0.025 M sucrose. [c] Experiment conducted with a feed solution containing 0.002 M methanol and 0.0001 M glycerol. Methanol/glycerol selectivity was 2.6 ± 0.9.

work showed that capping of a 5-bilayer PSS/PAH precursor film with 1.5 bilayers of PAA/PAH yields dramatic increases in Cl^-/SO_4^{2-}selectivity without greatly hindering Cl^- flux, so we attempted to use this strategy to enhance selectivity in neutral molecule transport. The flux of glycerol through 5 bilayers of PSS/PAH capped with 1.5 bilayers of PAA/PAH is about one-third of that through 6.5-bilayer PSS/PAH films, but glucose flux is 30-fold lower through the capped films. Thus, the overall glycerol/glucose selectivity increases from 6.4 to 75 when using the capping layers (Table 2). With films capped with 1.5 bilayers of PAA/PAH, the concentration of sucrose in the permeate is below the detection limit of our analysis ($\sim 2 \times 10^{-7}$ M), and thus, we can only establish a minimum glucose/sucrose selectivity, which is 200.

Methanol/glycerol selectivity with [PSS/PAH]$_5$ [PAA/PAH]PAA films (3.5) is significantly less than that for glycerol over glucose, indicating that the pores in capped membranes are still too large to effectively separate small molecules. This again suggests that the high selectivity in previous ion-transport studies was primarily due to electrostatic effects. The Cl^-/SO_4^{2-} selectivity of [PSS/PAH]$_5$[PAA/PAH]PAA films is 70,[41] even though SO_4^{2-} has a smaller Stokes' radius (0.23 nm) than glycerol.

The selectivity of capped membranes decreases dramatically when the polyelectrolyte films terminate in PAH rather than PAA (Table 2). Upon going from a 1.5-bilayer to a 2-bilayer PAA/PAH cap, glycerol/glucose selectivity decreases from 75 to 10, and methanol/glycerol selectivity decreases from 3.5 to 2.4. Presumably, the film with PAA as the terminal layer has a tighter structure than the film with PAH as the top layer. (This trend is opposite to that for PAH and PSS and may reflect the fact that carboxylates are less hydrated than sulfonates.[62]) Although selectivity among small molecules decreases when capped films terminate with PAH, such membranes still exhibit a selectivity of 130 for glucose over sucrose, and glucose flux through [PSS/PAH]$_5$[PAA/PAH]$_2$ films is 15-fold greater than that with a 1.5-bilayer PAA/PAH capping layer. Such wide variations in transport properties should be beneficial for developing membranes for specific applications.

Nanofiltration with PSS/PAH Membranes. Table 3 shows percent rejection values, selectivities, and water fluxes (in m^{3}m^{-2}d^{-1}) from NF experiments with 6.5- and 7-bilayer PSS/PAH membranes and solutions containing several neutral molecules. Percent rejection is defined by eq 1

$$\% \text{ rejection} = \left(1 - \frac{C_{\text{perm}}}{C_{\text{feed}}}\right) \times 100\% \qquad (1)$$

where C_{feed} is the concentration in the feed and C_{perm} is the concentration in the permeate.

Water flux through these films is 20−60% lower than that in our previously published results with 4.5- or 5-bilayer PSS/PAH membranes,[59] presumably because of the greater thickness of 6.5- and 7-bilayer films. However, water fluxes are still similar to those of commercial NF membranes.[63,64]

PSS/PAH membranes show impressive NF selectivities that correlate well with results from diffusion

(62) Davis, T. A.; Genders, J. D.; Pletcher, D. *A First Course in Ion Permeable Membranes*; The Electrochemical Consultancy: Romsey, U.K., 1997.

(63) Performance characteristics of some commercially available membranes can be found at www.dow.com/liquidseps/pc/nfe.htm.

(64) Bhattacharyya, D.; Williams, M. E.; Ray, R. J.; McCray, S. B. *Membrane Handbook*; Van Nostrand Reinhold: New York, 1992.

dialysis. In NF, selectivities are calculated according to eq 2

$$\text{Selectivity} = (100 - R_1)/(100 - R_2) \qquad (2)$$

where R_1 and R_2 represent percent rejections of two different compounds. Glucose/sucrose selectivities for 6.5-bilayer and 7-bilayer PSS/PAH membranes are 70 and 140, respectively, and the corresponding values in diffusion dialysis are 80 and 150. Methanol/glycerol and glycerol/glucose selectivities are also similar to those determined in diffusion dialysis. Compared to 7-bilayer PSS/PAH, 6.5-bilayer PSS/PAH membranes exhibit lower selectivities for both glycerol/glucose and glucose/sucrose. However, water fluxes through 7-bilayer and 6.5-bilayer films are about the same. If the higher selectivities of 7-bilayer films were due to tighter surface packing, we would expect to see a slightly lower water flux with these films. A small difference in water flux could, however, be obscured by the experimental error in our measurements.

Despite high selectivities, PSS/PAH membranes will probably not be useful for the separation of small organic molecules because of their high rejection values. As shown in Table 3, with 7-bilayer PSS/PAH membranes, methanol, glycerol, glucose and sucrose rejections are 70, 88, 98.3, and 99.99%, respectively. Nevertheless, these high rejections could be very beneficial in salt/sugar separations or removal of organic pollutants from water.[54] In the former case, rejection of sugars and high passage of salts should allow selective concentration of oligosaccharides.

The high rejection of sucrose resulted in permeate concentrations near the detection limit of our chromatograph. Because of this, we performed NF with a glycerol/glucose/sucrose solution that contained 0.025 M sucrose rather than 0.005 M sucrose (Table 3). Rejection of both glycerol and glucose increased with the higher sucrose concentration, presumably because sucrose blocked pores at the membrane surface. A decrease in water flux also suggests the presence of adsorbed sucrose, although increased osmotic pressure (9 psi) due to the higher sucrose concentration probably accounts for much of the flux reduction. Sucrose rejection was similar for 0.025 and 0.005 M feed solutions, but rejection was very high in both cases.

Theory for Modeling of Transport. Figure 2 shows schematically the concentration profile of a solute diffusing through a multilayer polyelectrolyte/porous alumina membrane. To model diffusion dialysis through such a membrane, we utilized Fick's first law (eq 3) in both the alumina and the polyelectrolyte film.

$$j_i = -D_i \frac{dc_i}{dx} \qquad (3)$$

In this equation, j_i represents solute flux, D_i is the solute diffusion coefficient in a particular medium, and dc_i/dx is the concentration gradient. Because flux is at steady state (see Figure 1 for evidence of steady-state transport), Fick's law can be rewritten as

$$j_i = -D_i \frac{\Delta c_i}{\Delta x} \qquad (4)$$

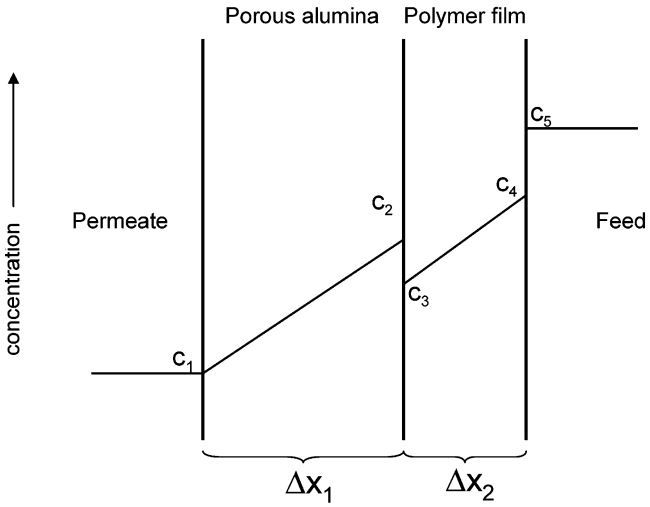

Figure 2. Schematic diagram of the analyte concentration profile in a membrane composed of a polyelectrolyte film on a porous alumina support: Δx_1, thickness of the porous support; Δx_2, thickness of the polyelectrolyte film; c_1, analyte concentration in the permeate; c_2, analyte concentration in the alumina support at the support−film interface; c_3, analyte concentration in the film at the support−film interface; c_4, analyte concentration in the film at the film−solution interface; c_5, analyte concentration in the feed.

where Δx is the thickness of either the porous alumina or the polyelectrolyte film and Δc_i represents the total drop in concentration within either layer. There are also concentration changes at the alumina/polyelectrolyte and polyelectrolyte/feed interfaces due to partitioning into the MPM. (Because the pores in the alumina are large (20−200 nm), there should be no concentration change at the alumina/permeate interface.) With the assumption that the polyelectrolyte film behaves like an assembly of small cylindrical pores,[65−68] eq 5 describes the relationship between the concentration at the surface of the polyelectrolyte film, c_4, and the concentration in the feed, c_5 (Figure 2). The partition coefficient, Φ, is a function of λ, the ratio of Stokes' radius to pore radius. A similar relationship should exist at the polyelectrolyte/alumina (c_3/c_2) interface.

$$\Phi = c_4/c_5 = c_3/c_2 = (1 - \lambda)^2 \qquad (5)$$

Assuming that the concentration in the permeate phase, c_1, is negligible compared to c_2, we can calculate c_2 from the experimental flux value using eq 6. We obtained D_1, the diffusion coefficient in the porous alumina, from diffusion dialysis data with a bare porous alumina support, and Δx_1 is thickness of the alumina (∼60 μm).

$$c_2 = j_i \Delta x_1 / D_1 \qquad (6)$$

For transport through the polyelectrolyte film, substitution of eqs 5 and 6 into eq 4, plus rearrangement, yields the expression for flux in eq 7.

$$j_i = \frac{c_5}{\dfrac{\Delta x_2}{D_2(1 - \lambda)} + \dfrac{\Delta x_1}{D_1}} \qquad (7)$$

However, D_2, the diffusion coefficient in the MPM, is a

function of the hindrance factor for diffusion in small pores, $K_{i,d}$, the film porosity, ϵ, and the diffusion coefficient in free solution, D_{inf}, as shown in eq 8.[55]

$$D_2 = D_{inf} K_{i,d} \epsilon \tag{8}$$

Using correlations for $K_{i,d}$ as a function of λ (see below), one can write the flux j_i through the MPM in terms of two variables, λ and ϵ. To estimate film porosity, we utilized measurements of water flux in NF. Assuming that all the pores in a film have the same radii, volume flux in NF can be described by eq 9

$$J_v = \frac{\epsilon r^2 \Delta P}{8 \eta \tau \Delta x} \tag{9}$$

where J_v is the volume flux, r is the pore radius, ΔP is the pressure drop across the film, η is the solvent viscosity, and τ is the pore tortuosity. (For straight cylindrical pores, the tortuosity is equal to unity.) With water-flux data from NF and solute-flux data from diffusion dialysis, eqs 7 (with substitution of eq 8) and 9 can be solved iteratively for r and ϵ if the radius of the solute is known. In our actual calculation of r, we first assumed a value of r and calculated ϵ from eq 9 and D_2 from eq 8 and the correlations given below for $K_{i,d}$. Finally, we calculated flux from eq 7. We optimized the value assumed for r to minimize the sum of least squares of percent error in the fluxes of methanol, glycerol, glucose, and sucrose.

In the case of NF, the expression for solute flux contains both diffusive and convective terms. The treatment that we followed to simulate transport is similar to that developed by Bowen et al.[55] Addition of convection to Fick's law yields eq 10, where J_v is the volume flux of the solvent.

$$j_i = -D_i \frac{dc_i}{dx} + K_{i,c} c_i J_v \tag{10}$$

The hindered nature of convection and diffusion inside membrane pores is accounted for by $K_{i,c}$, the hindrance factor for convection, and $K_{i,d}$ (eq 8 for D_2), the hindrance factor for diffusion, which are functions of λ. If one assumes a homogeneous velocity across very small membrane pores, $K_{i,d}$ and $K_{i,c}$ are respectively equivalent to $K^{-1}(\lambda,0)$, the enhanced drag coefficient, and $G(\lambda,0)$, the lag coefficient.[55,67] Bungay and Brenner fitted the enhanced drag and lag coefficients to eqs 11 and 12.[69,70] Other correlations for drag and lag coefficients gave similar results in our simulations.[55,69]

$$K^{-1}(\lambda,0) = 6\pi/\left\{\frac{9}{4}\pi^2\sqrt{2}(1-\lambda)^{-2.5}\left[1 - \frac{73}{60}(1-\lambda) + \frac{77293}{50400}(1-\lambda)^2\right] - 22.5083 - 5.6117\lambda - 0.3363\lambda^2 - 1.216\lambda^3 + 1.647\lambda^4\right\} \tag{11}$$

$$G(\lambda,0) = \left\{\frac{9}{4}\pi^2\sqrt{2}(1-\lambda)^{-2.5}\left[1 + \frac{7}{60}(1-\lambda) - \frac{2227}{50400}(1-\lambda)^2\right] + 4.0180 - 3.9788\lambda - 1.9215\lambda^2 + 4.392\lambda^3 + 5.006\lambda^4\right\} \frac{K^{-1}(\lambda,0)}{12\pi} \tag{12}$$

Integration of eq 10 over the polyelectrolyte film with the boundary conditions listed in eq 13 ($c_{i,f}$ and $c_{i,p}$ are the solute concentrations in the feed and permeate, respectively) yields the expression for rejection, R, in eq 14. In this equation, the Peclet number, Pe_m is defined as shown in eq 15.

$$c_{i,x=0} = \Phi\, c_{i,f} \text{ and } c_{i,x=\Delta x} = c_{i,p} \tag{13}$$

$$R = 1 - \frac{c_{i,p}}{c_{i,f}} = 1 - \frac{K_{i,c}\Phi}{1 - \exp(-Pe_m)(1 - K_{i,c})} \tag{14}$$

$$Pe_m = \frac{K_{i,c}}{K_{i,d}} \frac{J_v \Delta x}{D_{i,\infty}\epsilon} \tag{15}$$

Eqs 14 and 15 provide an expression for rejection as a function of λ and ϵ.

In the actual procedure for determining the porosity and pore radius from NF data, we first assumed a value for pore size and calculated porosity from eq 8 and the hindrance factors for both diffusion and convection using eqs 10 and 11. Subsequently, we calculated rejection with eq 13. Iterations on this procedure yielded a best-fit pore radius through minimization of the sum of least squares for the percent error in (1 − rejection) for methanol, glycerol, and glucose.

We note that for cross-flow NF, we assumed partition equilibrium only at the feed-side interface. The polyelectrolyte/alumina interface is not stirred so we assumed that the concentration on the alumina side of this interface is the same as the concentration in the polyelectrolyte. We also neglected mass-transport resistance due to the alumina support. This is an appropriate assumption in NF because water flux through bare alumina is >100 times larger than flux through PSS/PAH-coated alumina. In diffusion dialysis, however, the alumina support provides a significant resistance to mass transport.

Determination of Effective Pore Sizes. The models described above allow estimation of effective pore sizes in polyelectrolyte films, and these parameters will be important for prediction of selectivity and flux in specific separations. Table 4 shows simulated fluxes for diffusion dialysis and the important variables used to calculate these fluxes. Minimization of the percent error in the fluxes of the different solutes gave an effective pore radius of 0.53 nm and a porosity of 1.8%. (Note that porosity is low because we assumed a tortuosity of 1, and calculated porosity is directly proportional to the value assumed for tortuosity. Neutron reflectivity experiments suggest that multilayer polyelectrolyte films contain 40% water, so we would expect a much higher porosity.[31]) Calculated fluxes of all four solutes were within at least 32% of the measured values. However, effective pore size depends greatly on the value of D_{inf} chosen for the calculation. We utilized the effective

(65) Wang, X. L.; Tsuru, T.; Togou, M.; Nakao, S.; Kimura, S. *J. Chem. Eng. Jpn.* **1995**, *28*, 186−192.
(66) Wang, X. L.; Tsuru, T.; Togou, M.; Nakao, S.; Kimura, S. *J. Membr. Sci.* **1997**, *135*, 19−32.
(67) Bowen, W. R.; Mukhtar, H. *J. Membr. Sci.* **1996**, *112*, 263−274.
(68) Nakao, S.; Kimura, S. *J. Chem. Eng. Jpn* **1982**, *15*, 200−205.
(69) Deen, W. M. *AIChE J.* **1987**, *33*, 1409−1425.
(70) Bungay, P. M.; Brenner, H. *Int. J. Multiphase Flow* **1973**, *1*, 25−56.

Table 4. Parameters and Fluxes (mol cm^{-2} s^{-1}) Relevant to the Simulation of Diffusion Dialysis through a 7-Bilayer PSS/PAH Membrane Assuming $r = 5.28 \times 10^{-8}$ cm[a]

	λ	$(1-\lambda)^2$	D_{inf}(cm^{2}s^{-1})	D_2(cm^{2}s^{-1})	J calculated	J measured
methanol	0.3	0.49	2.14×10^{-6}	1.60×10^{-8}	6.3×10^{-8}	6.0×10^{-8}
glycerol	0.49	0.26	1.57×10^{-6}	4.84×10^{-9}	8.0×10^{-10}	8.7×10^{-10}
glucose	0.67	0.11	1.08×10^{-6}	9.87×10^{-10}	1.5×10^{-10}	1.1×10^{-10}
sucrose	0.89	0.012	7.98×10^{-7}	3.70×10^{-11}	7.2×10^{-12}	7.3×10^{-12}

[a] A porosity of 1.8% was calculated from eq 8 using nanofiltration data at 70 psi that yielded a water flux of 0.001 cm^3 cm^{-2} s^{-1}. The polyelectrolyte film thickness was assumed to be 30 nm based on ellipsometric measurements.

Table 5. Parameters and Rejections Calculated in the Simulation of Nanofiltration with a 7-Bilayer PSS/PAH Membrane Assuming $r = 4.2 \times 10^{-8}$ cm[a]

	λ	$(1-\lambda)^2$	K^{-1}	$K_{i,c}$	calculated % rejection	measured % rejection
methanol	0.374	0.392	0.31	0.89	61.4	70 ± 5
glycerol	0.619	0.145	0.078	0.76	87.5	88 ± 2
glucose	0.845	0.024	0.0067	0.60	98.5	98.3 ± 0.2
sucrose	>1				100	99.99 ± 0.01

[a] A porosity of 2.8% was calculated from eq 8 using nanofiltration data at 70 psi that yielded a water flux of 0.001 cm^{3}cm^{-2}s^{-1}. The polyelectrolyte film thickness was assumed to be 30 nm.

diffusion coefficient (uncorrected for porosity) in porous alumina as the value of D_{inf}. If we correct this value for the alumina porosity determined from NF experiments (21%), the calculated pore size in the polyelectrolyte film decreases to 0.45 nm and porosity increases to 2.5%.[71] We utilized the uncorrected value for the diffusion coefficient because we thought that diffusion through the film would not occur to nonporous areas of the alumina surface. (This assumption implies that lateral diffusion at the polyelectrolyte/alumina interface is insignificant.) The calculated diffusion coefficient, D_2, for sucrose (MW = 342) is similar to that measured by Ibarz et al. for fluorescein (MW = 332) diffusion through annealed polyelectrolyte capsules.[72]

Simulation of NF (Table 5) resulted in a pore size of 0.42 nm and a porosity of 2.8%. Calculated rejections were within 12% of measured values, which is fairly remarkable considering the simplicity of the transport model. The simulations assume a uniform pore size, while, in fact, there is certainly a distribution of pore sizes that results from the complicated packing of the polymers. Additionally, pores need not be cylindrical, and the radius of a single pore may not be homogeneous. Thus, effective pore sizes are only rough approximations. This may explain why a small amount of sucrose passes through the membrane even though its Stokes' radius is larger than the effective pore radius. Still, the simulations model the data well, and the agreement between nanofiltration and diffusion dialysis simulations is quite good. Additionally, the effective pore sizes should allow estimation of the rejections of other solutes. The calculated pore size in NF is only 0.1 nm less than the value from diffusion dialysis, and this small difference may reflect the approximate nature of the simulations or the choice of diffusion coefficient in the diffusion dialysis calculation. Compaction due to the pressure applied in NF could also decrease pore sizes.

Effective pore sizes are consistent with the fact that the approximate molecular weight cutoff (90% rejection in NF) of these membranes is around 92, the molecular weight of glycerol. The Stokes' radius of glycerol is 0.26 nm, and molecules larger than this should be highly rejected from the membrane, primarily due to the partition coefficient, which is a function of the ratio of Stokes' radius to pore radius (eq 5). In fact, the NF model suggests that partitioning is the primary factor behind selectivity with the molecules examined, although there is a small effect from hindered convection. (Diffusion is not a major source of transport in the nanofiltration studies, so differences in diffusion coefficients have little effect on selectivity.)

One of the reasons for performing this work was to determine if there was a size-based selectivity in ion separations, e.g., Cl^- and SO_4^{2-}. Because the Stokes' radii of these ions are significantly less than the pore radius, size selectivity should be <2 with PSS/PAH membranes. However, other polyelectrolyte systems may pack more tightly and allow for size discrimination among small ions. Additionally, electrostatic interactions between ions and polyelectrolytes can result in selective diffusion, as shown by Farhat and Schlenoff.[39,40] Our future work aims at controlling pore size in MPMs by carefully selecting constituent polyelectrolytes.

Conclusions

MPMs are highly selective for neutral molecules in both diffusion dialysis and NF. These membranes demonstrate glucose/sucrose selectivities as high as 150, and size exclusion is the main factor behind such selectivities. Modeling of solute and solvent fluxes as well as rejection values suggests that PSS/PAH membranes contain pores with radii of 0.4−0.5 nm. The high rejections of glucose and sucrose by PSS/PAH membranes along with a high water flux suggest that these materials may be applicable in salt/sugar separations or removal of organic pollutants from water. In contrast to neutral molecules, however, selective transport of small ions such as Cl^- and SO_4^{2-} through PSS/PAH films should not be based on size because the Stokes' radii of these ions are significantly smaller than film pores.

Acknowledgment. We thank the Department of Energy Office of Basic Energy Sciences for financial support.

CM034559K

(71) After correcting for porosity, diffusion coefficients measured in porous alumina are about 60% of those literature values listed in Table 1. This may reflect the fact that diffusion coefficients in alumina were not measured at infinite dilution. If the diffusion coefficients in Table 1 are used in simulations, we obtain a pore radius of 0.44 nm and a porosity of 2.6%. The choice of diffusion coefficients has little effect on simulations of NF, however.

(72) Ibarz, G.; Dähne, L.; Donath, E.; Möhwald, H. *Chem. Mater.* **2002**, *14*, 4059−4062.